J Bioenerg Biomembr (2010) 42:371–379
DOI 10.1007/s10863-010-9308-5

The oxoglutarate/malate carrier of rat brain mitochondria operates by a uniport exchange mechanism

A. De Palma · G. Prezioso · A. Spagnoletta · G. Genchi · V. Scalera

Published online: 4 September 2010

Abstract Here, the oxoglutarate carrier, already isolated from various sources and described in the literature, has been purified from rat brain and reconstituted in proteoliposomes for an accurate kinetic study. The rate of uptake of labelled oxoglutarate and malate has been measured in various conditions, essentially in double substrate experiments. The data so obtained fit the hypothesis that the carrier operates by a uniport-exchange mechanism and provide significant values for the kinetic constants and the equilibrium constants implied in the process. Their analysis leads to the conclusion that the carrier is maximally efficient in the exchange between external malate and internal oxoglutarate, as required by the malate/aspartate shuttle, which should be the main role of the oxoglutarate carrier in brain mitochondria.

Keywords Mitochondria · Oxoglutarate carrier · Rat brain · Exchange by uniport mechanism

Abbreviations

PIPES	1,4-piperazine-diethanesulphonic acid
HEPES	4-(2-hydroxyethyl)-1-piperazineethanesulfonic acid
PLP	pyridoxal 5′-phosphate
SDS-PAGE	sodium dodecyl sulfate polyacrylamide gel electrophoresis
OGC	oxoglutarate carrier

A. De Palma · G. Prezioso
Dipartimento Farmaco-biologico, Università degli Studi di Bari, Bari, Italia

A. Spagnoletta · V. Scalera (✉)
Dipartimento di Fisiologia Generale ed Ambientale, Università degli Studi di Bari, via Amendola 165/A, 70126 Bari, Italia
e-mail: v.scalera@biologia.uniba.it

G. Genchi
Dipartmento Farmaco-Biologico, Università della Calabria, Arcavacata di Rende, Cosenza, Italia

Introduction

The oxoglutarate carrier (OGC) is a protein of the inner mitochondrial membrane whose primary function is to mediate a oxoglutarate/malate exchange between the cell cytoplasm and the mitochondrial matrix, playing an important role in metabolic processes such as the malate/aspartate shuttle, the isocitrate/oxoglutarate shuttle and gluconeogenesis. The carrier protein has been purified from the heart (Bisaccia et al. 1985; Bolli et al. 1989) and liver (Bisaccia et al. 1988) and the definition of its primary structure (Runswick et al. 1990) led to classify it as a member of the largest family of mitochondrial carriers (Walker and Runswick 1993). This family consists of protomers with a molecular weight of about 30–35 kDa, whose sequence is divided into three homologous domains of about 100 amino acids. Each domain contains two hydrophobic α-helixes that span the membrane (Palmieri 2004). Kinetic characterization of the transport mechanism has been reported for the OGC from heart after reconstitution in proteoliposomes. From the kinetic pattern a sequential exchange mechanism has been deduced, implying that one internal and one external substrate molecule form a ternary complex with the carrier before transport occurs (Indiveri et al. 1991).

In this study we describe the purification of the OGC from rat brain and its reconstitution in proteoliposomes by means of a modified procedure (Spagnoletta et al. 2008) that leads to a

more reliable performance of the kinetic investigation. The kinetic data so obtained support the hypothesis of a alternative to the sequential mechanism described as exchange by uniport, in analogy to what has already been found for the citrate carrier in rat liver mitochondria (De Palma et al. 2005). In such a hypothesis, the following scheme describes the interactions of the carrier with its substrates (indicated as A and B) when both are present:

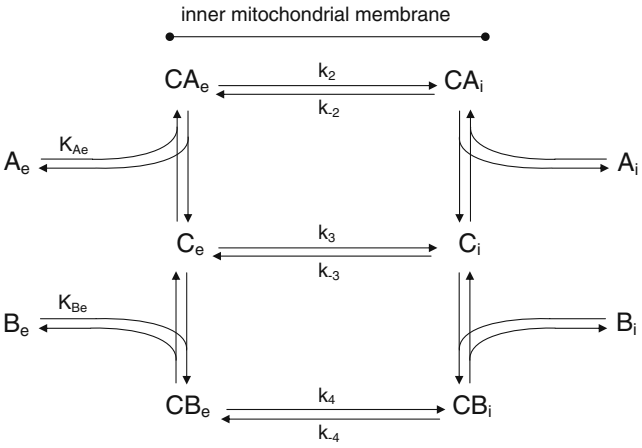

For a homologous exchange the mechanism is analytically described by an equation where the initial rate of uptake of a labelled substrate (e.g. [^{14}C]oxoglutarate) into liposomes is expressed as a function of the external and internal concentrations of the substrate itself (A_e and A_i respectively), and is as follows:

$$\vec{v} = k_2 \cdot CA_e = k_2 \cdot C_T \cdot \frac{k_{-2}A_i + k_{-3}K_{Ai}}{(k_{-2}+k_2)A_i + (k_{-3}+k_2)K_{Ai}} \cdot \frac{A_e}{A_e + \frac{(k_{-2}+k_3)A_i+(k_{-3}+k_3)K_{Ai}}{(k_{-2}+k_2)A_i+(k_{-3}+k_2)K_{Ai}} K_{Ae}}$$

$$= \vec{V}_M \cdot \frac{A_e}{A_e + \vec{K}_M} \quad (1)$$

where

$$\vec{V}_M = k_2 \cdot C_T \cdot \frac{k_{-2}A_i + k_{-3}K_{Ai}}{(k_{-2}+k_2)A_i + (k_{-3}+k_2)K_{Ai}} \quad (1a)$$

and

$$\vec{K}_M = \frac{(k_{-2}+k_3)A_i + (k_{-3}+k_3)K_{Ai}}{(k_{-2}+k_2)A_i + (k_{-3}+k_2)K_{Ai}} K_{Ae} \quad (1b)$$

K_{Ae} and K_{Ai} are the dissociation constants of the carrier-substrate complexes on the external and internal side respectively, k_2 and k_{-2} are the kinetic constants of the rearrangement steps of the carrier-substrate complex moving the substrate from outside to inside and *vice versa*, while k_3 and k_{-3} are referred to the analogous rearrangements of the carrier with its free binding site. CA_e represents the concentration of the carrier-substrate complex with the substrate bound on the external side, and C_T the total concentration of the carrier in its various forms. The equation is obtained by considering the interactions of the substrate with the carrier as fast steps of the transport process (then ruled by the dissociation constants), and conversely the rearrangements of the carrier in its various forms as slow, and hence rate determining, steps (ruled by their kinetic constants).

The presence of a second substrate B (malate, in this study) in substitution of, or in addition to, oxoglutarate inside or outside the proteoliposomes leads to different forms of the velocity equation, containing additional kinetic and dissociation parameters referred to B.

Materials and methods

Chemicals

[^{14}C]oxoglutarate and [^{14}C]malate were purchased from Perkin-Elmer Life Sciences; hydroxylapatite (Bio-gel HTP) and Amberlite Bio-Beads SM-2 from Bio-Rad; Triton X-100, acrylamide and N,N′-methylenebisacrylamide from Serva; egg-yolk phospholipids (phosphatidylcholine from fresh turkey egg-yolk) from Fluka; Matrex Gel Orange from Amicon (Beverly, MA); cardiolipin, Pipes, Hepes, SDS and asolectin from Sigma; celite 535 from Roth and Sephadex G-75 from Pharmacia. All other chemicals used were of analytical grade.

Purification of the OGC

Rat brain mitochondria, prepared with standard procedures, were solubilized with 3% Triton X-100 (w/v), 20 mM Na_2SO_4, 1 mM EDTA and 10 mM Pipes, pH 7.0 (buffer 1) at a final protein concentration of 10 mg/ml. After 10 min at 4 °C, the mixture was centrifuged at 15,000 g for 15 min and 100 μl of supernatant, supplemented with 4 mg/ml of cardiolipin in buffer 1, were applied to cold hydroxylapatite/celite (5:1) columns (pasteur pipettes, 0.6 g of dry material) and eluted with buffer 1. The first 0.6 ml eluted from two hydroxylapatite/celite columns were collected and applied on cold Matrex Gel Orange column (pasteur pipettes filled with 1 ml of resin), pre-equilibrated with 4 ml of 0.1% Triton X-100, 10 mM Na_2SO_4, 1 mM EDTA and 5 mM Pipes, pH 7.0 (buffer 2). Elution was performed with 4 ml of buffer 2, followed by 1.6 ml of the same buffer with added 2 mg/ml asolectin (asolectin buffer). Fractions of 0.8 ml were collected. Pure OGC was present in the second fraction eluted with the asolectin buffer and the SDS-polyacrylamide gel electropho-

resis shows a single protein band with an apparent molecular mass of 35 kDa (Fig. 1 line E). All the operations were performed at 4 °C. Prior to addition of sample, the Matrex Gel Orange had been washed sequentially with 4 ml of 8 M urea, 4 ml of distilled water and 4 ml of buffer 2. The urea washing was carried out at room temperature, whereas all subsequent washes were performed at 4 °C.

Reconstitution of the OGC in liposomes

Protein eluates were reconstituted into liposomes by removing the detergent with hydrophobic chromatography using a micro-batchwise method (Spagnoletta et al. 2008). In this procedure, the mixed micelles containing detergent, protein and phospholipids were kept in a eppendorf tube on a rotating plate stirrer, in the presence of detergent removing Amberlite Bio-Beads SM-2. The composition of the initial mixture used for reconstitution was: 200 µl of the eluates of the different chromatography columns, 100 µl of 10% (w/v) Triton X-114, 80 µl of 10% (w/v) egg yolk phospholipids in the form of liposomes, oxoglutarate at the indicated concentrations, 200 µl of 10 mg/ml asolectin and 10 mM Pipes, pH 7.0, in a final volume of 700 µl. After vortex-mixing, this mixture was added into the Eppendorf tube (2 ml) filled with Amberlite Bio-Beads SM-2 (0.4 g) and after 480 total revolutions (32 rpm) by rotating plate stirrer, the proteoliposomes were recovered by gently aspiration.

All the operations were perfomed at room temperature.

Transport measurements

The external substrate of the proteoliposomes suspention was removed by passing 650 µl of the proteoliposomes through a Sephadex G-75 column (0.7×15 cm), pre-equilibrated with 50 mM NaCl/10 mM Pipes (pH 7.0). The first 600 µl of turbid eluate from the Sephadex G-75 column were collected, 100 µl transferred to reaction vessels and used for transport measurements by the inhibitor stop method (Palmieri et al. 1995). Transport was initiated by adding 10 µl of [^{14}C]oxoglutarate or [^{14}C]malate at the indicated concentrations and stopped, after the desired time interval, by adding 10 µl 350 mM PLP as inhibitor. In control samples, the inhibitor was added together with the labelled substrate at time zero. Each sample was run in duplicate. The assay temperature was 25 °C. The external radioactivity was removed by passing the samples (100 µl) through a Sephadex G-75 column (0.6×8 cm). The liposomes, eluted with 1.2 ml of 50 mM NaCl, were collected in 4 ml of scintillation mixture, mixed by a vortex and counted. The transport activity was calculated by subtracting the respective control sample from the experimental values.

Other methods

Polyacrylamide slab-gel electrophoresis of acetone-precipitated proteins was performed in the presence of 0.1% SDS by the method of Laemmli (Laemmli 1970). A minigel system was used. Gel sizes were 8×10 cm (1.5 mm thick). The stacking gel contained 5% (w/v) polyacrylamide and the separation gel contained 17.5% (w/v) polyacrylamide, with an acrylamide/bisacrylamide ratio of 38:1. Staining was performed by the silver nitrate method (Morrissey 1981).

Protein was determined by the Lowry method modified for the presence of non-ionic detergents (Dulley and Grieve 1975). All the samples used for protein determination were subjected to precipitation with acetone and redissolved in 1% (w/v) SDS.

Results

The ability of the reconstituted OGC of rat brain mitochondria to catalyze the transport of its substrates across the

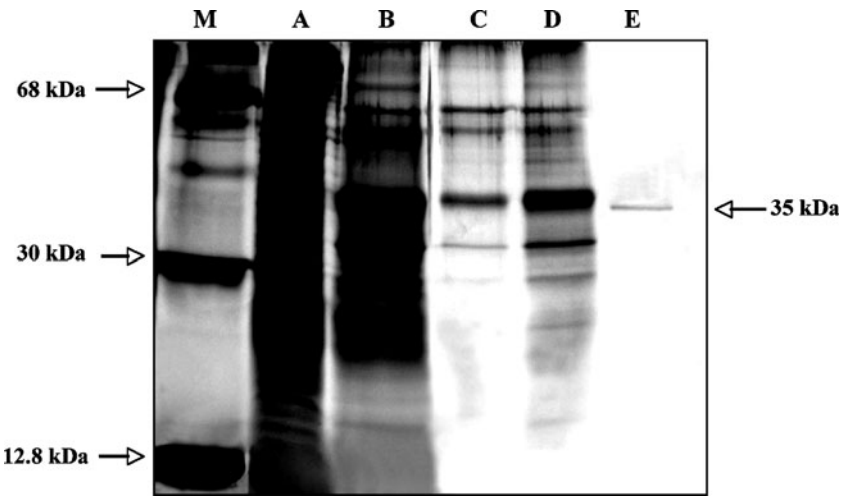

Fig. 1 Purification of OGC from rat brain mitochondria. SDS gel electrophoresis of eluates obtained by hydroxylapatite/celite chromatography and by Matrex Gel Orange A. Lane M, marker proteins (bovine serum albumin, carbonic anhydrase and Cyt c); lane A, mitochondrial extract; lane B, hydroxylapatite/celite eluate; lane C, Matrex Gel Orange A fraction eluted with buffer 2; lane D and E, first and second Matrex Gel Orange A fractions eluted with asolectin buffer. Other conditions were as described in Purification of the OGC section

proteoliposome is shown in a typical time-course experiment (Fig. 2) where the uptake of [^{14}C]oxoglutarate (A) and [^{14}C]malate (B) into proteoliposomes loaded with unlabelled oxoglutarate is measured as a function of time. It can be observed that both processes can be considered linear for several minutes from the beginning, and that they tend to reach equilibrium after about more than 1 hour. The linearity of the initial part of the time curves permits the measurement on the activity of the carrier protein as the initial transport rate, reported as taken up nmoles/min•mg protein.

For a first characterization of the carrier activity an analysis of the pH and temperature dependence has been performed. The pH dependency (Fig. 3A) shows a quite broad maximum between 6 and 7, with a significant decline already at pH 7.5. The dependence on temperature has been evaluated in the range from 5 °C to 35 °C. The Arrhenius plot of the data (Fig. 3B) allows us to measure an activation energy value of 13.2 kcal/mol, in the same order of magnitude of the values found for other mitochondrial carriers.

In order to compare the specificity of the carrier with that of its homologues described in the literature in both intact mitochondria and in proteoliposomes from different sources, we have measured the oxoglutarate uptake by proteoliposomes loaded with various molecules. The results of this analysis are shown in Table 1 and clearly indicate a strict similarity with homologous transport systems: besides oxoglutarate itself malate is the most effective in promoting the substrate influx, whereas among the others only succinate and malonate have a lesser but significant effect.

That malate is actually a substrate for the OGC is confirmed by the experiment in Fig. 4 where, added in the external medium, malate behaves as a competitive inhibitor with respect to the labelled oxoglutarate. A similar result has been obtained with succinate (not shown).

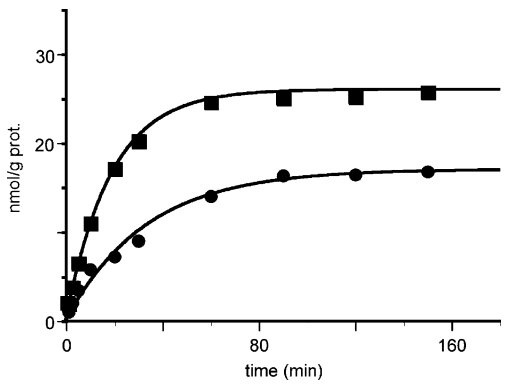

Fig. 2 Time-course of [^{14}C]oxoglutarate and [^{14}C]malate uptake in reconstituted liposomes. 0.1 mM [^{14}C]oxoglutarate or (■) 0.1 mM [^{14}C]malate (●) was added at zero time to reconstituted liposomes containing 10 mM oxoglutarate. Transport was stopped at the indicated times and the intraliposomal radioactivity was measured

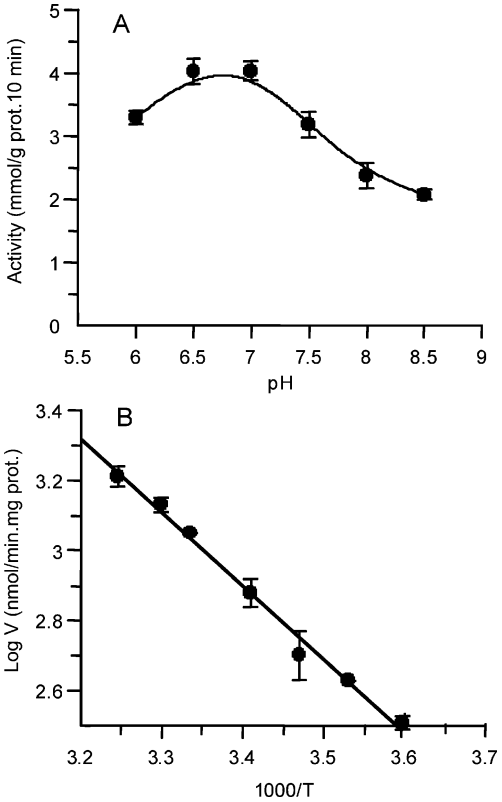

Fig. 3 **a** Effect of the pH on the reconstituted oxoglutarate carrier activity. The proteoliposomes contained 10 mM oxoglutarate and the transport was started by adding 0.1 mM [^{14}C]oxoglutarate. The reconstitution and the transport were performed at the indicated pH values. **b** Arrhenius plots of oxoglutarate uptake by purified OGC reconstituted in proteoliposomes. [^{14}C]oxoglutarate (0.1 mM) was added to proteoliposomes containing 10 mM oxoglutarate and incubated for 1 min at the indicated temperatures. The rates of exchange were measured. The means ± S.E. of three experiments are reported

Verification of our hypothesis of kinetic mechanism by uniport exchange requires in-depth evaluation of the dependence of transport activity on the concentration of external and internal substrates, in order to fit the experimental data to equations such as (1), that describe the proposed mechanism and consequently to derive consistent values for the parameters present in the equations.

To this aim a "double substrate" kinetic approach has been performed under different experimental conditions. Firstly, the homologous oxoglutarate/oxoglutarate exchange was examined, by using four different concentrations of external labelled oxoglutarate to three different concentrations of internal oxoglutarate. Figure 5 reports the activity data of a typical experiment, in double reciprocal plots with respect to the external substrate concentration. Three straight lines are obtained, each representing an internal substrate concentration, that tend to meet at a common point in the double negative quadrant of the

Table 1 Dependence on internal substrate of oxoglutarate transport in reconstituted liposomes

Internal substrate	Oxoglutarate transport (mmoli/10 min g prot.$^{-1}$)
None (Cl^-present)	0.071±0.026
oxoglutarate	7.099±0.011
L-Malate	6.354±0.821
Succinate	4.520±0.094
Malonate	3.535±0.356
Oxoadipate	0.827±0.345
Citrate	0.350±0.004
ATP	0.210±0.001
Adipate	0.204±0.053
Glutarate	0.164±0.006
Phosphate	0.110±0.004
Pyruvate	0.098±0.003
Glutamate	0.072±0.002
Fumarate	0.050±0.089

The reconstitution mixture contained each of the indicated substrates at 10 mM. Transport was initiated by adding 0.1 mM [^{14}C] oxoglutarate. The results are the means ± S.E. of four different experiments

Cartesian plane. These simple data already rule out the pure ping-pong mechanism, as will be discussed. More information can be obtained from the saturation rate and K_M values extrapolated for each line: second order plots have been traced for both V_M and K_M as functions of the internal substrate concentration (Fig. 6). They may fit to Eqs. (1a) and (1b) respectively, that describe two hyperbola. The parameters of such curves (intercepts with the two axis,

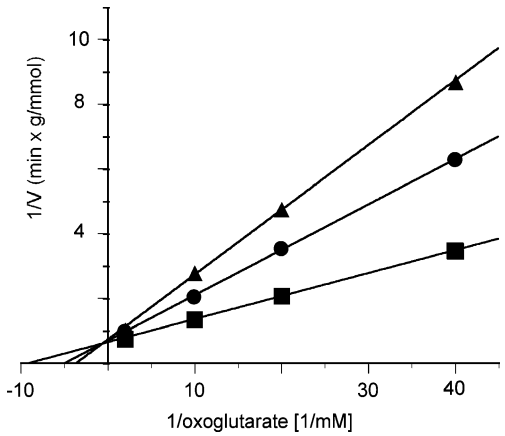

Fig. 4 Competitive inhibition of the oxoglutarate transport activity by malate. Double reciprocal plot showing the dependence of uptake rate on external concentrations. [^{14}C]oxoglutarate was added at the concentrations of 0.025, 0.05, 0.1 and 5 mM to proteoliposomes containing 9 mM oxoglutarate in absence (■) and in presence of external 0.27 mM (●) and 0.54 mM (▲) malate. The rate of uptake is measured in 2 min

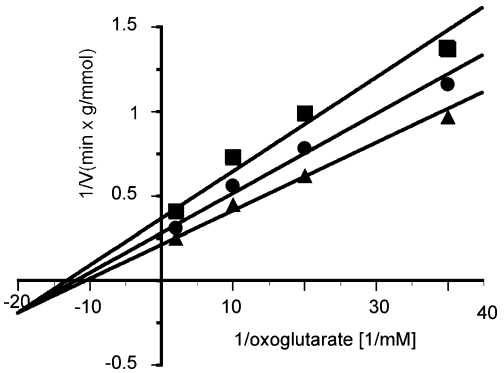

Fig. 5 Two-substrate analysis of the influx oxoglutarate in the presence of internal oxoglutarate, catalyzed by the reconstituted OGC. Double reciprocal plot showing the dependence of the uptake rate on external concentrations. [^{14}C]oxoglutarate was added at the concentrations of 0.025, 0.05, 0.1 and 0.5 mM to proteoliposomes containing 3 (■), 6 (●) and 9 mM (▲) oxoglutarate. The rate of uptake is measured in 2 min

asymptotes) are different combinations of the constants present in the general Eq. (1) and hence their traces condition each other.

The same data have been used to report the activities as functions of internal oxoglutarate, at four different concentrations of the external substrate. Four curves are obtained that do not show a tendency to meet the origin. These curves should be described by a different elaboration of Eq.

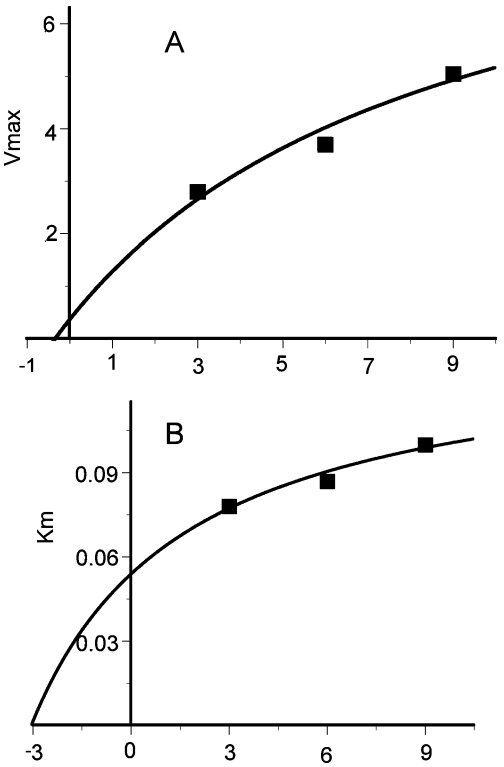

Fig. 6 Second-order plots of the data of Fig. 5. Dependence of the V_{max} (**a**) and K_m (**b**) on the internal oxoglutarate concentrations

(1), with A_i as the independent variable and A_e as a parameter:

$$\vec{v} = \vec{V}_M \cdot \frac{A_i + \vec{I}}{A_i + \vec{K}_M} \tag{2}$$

where

$$\vec{I} = \frac{k_{-3}}{k_{-2}} K_{Ai}$$

$$\vec{V}_M = k_2 \cdot C_T \cdot \frac{k_{-2} A_e}{(k_{-2} + k_2)A_e + (k_{-2} + k_3)K_{Ae}}$$

and (2a)

$$\vec{K}_M = \frac{(k_{-3} + k_2)A_e + (k_{-3} + k_3)K_{Ae}}{(k_{-2} + k_2)A_e + (k_{-2} + k_3)K_{Ae}} K_{Ai}$$

According to Eq. (2), the curves meet at a point on the negative side of the abscissa (-I). Actually, the experimental points satisfactorily fit such a pattern (Fig. 7). Clearly, in this case double reciprocal plots are not linear and do not provide further information. In analogy to Fig. 6, second order plots can be traced for V_M and K_M (Fig. 8) with respect to external oxoglutarate concentration, that should be described by the equations in (2a). Also in this case, we are dealing with hyperbola and the tracing of the plots is linked to the significance of their parameters.

The data shown in Figs. 5, 6, 7 and 8 allowed a calculation of significant values for the kinetic constants k_i

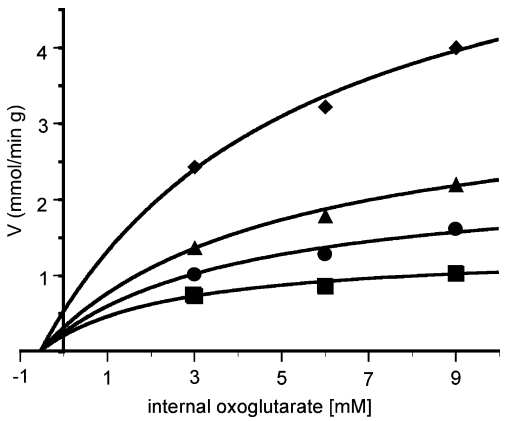

Fig. 7 Replot of data of Fig. 5. Dependence of the uptake rate of oxoglutarate in proteoliposomes on internal oxoglutarate concentrations. The concentrations of the countersubstrate were as follows: 0.5 (♦), 0.1 (▲), 0.05 (●), 0.025 (■) mM

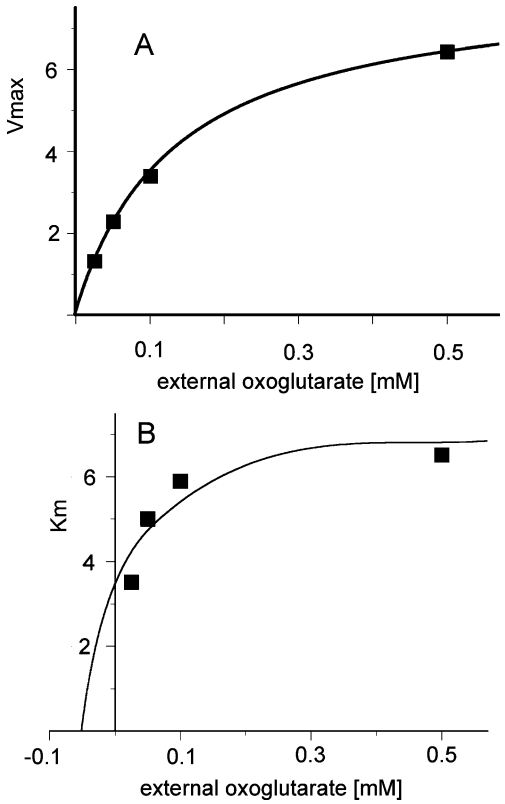

Fig. 8 Second-order plots of the data of Fig. 7. Dependence of the V_{max} (**a**) and K_m (**b**) on the external oxoglutarate concentrations

and the dissociation constants K_{Ae} and K_{Ai}, as will be seen in the Discussion section.

The malate/oxoglutarate exchange has also been analyzed by double substrate experiments by following the influx of labelled malate. It is easy to deduce that such exchange should be described by an equation strictly similar to (1) but with the external malate concentration expressed as B_e (instead of A_e), and hence K_{Be} instead of K_{Ae} and the kinetic constant k_4 instead of k_2.

$$\vec{v} = \vec{V}_M \cdot \frac{B_e}{B_e + \vec{K}_M} \tag{3}$$

where

$$\vec{V}_M = k_4 \cdot C_T \cdot \frac{k_{-2}A_i + k_{-3}K_{Ai}}{(k_{-2}+k_4)A_i + (k_{-3}+k_4)K_{Ai}}$$

and (3a)

$$\vec{K}_M = \frac{(k_{-2}+k_3)A_i + (k_{-3}+k_3)K_{Ai}}{(k_{-2}+k_4)A_i + (k_{-3}+k_4)K_{Ai}} K_{Be}$$

Figures 9 and 10 show the results of such an experiment in analogy to Figs. 5 and 6. Also in this case kinetic constants and dissociation constants have been evaluated by

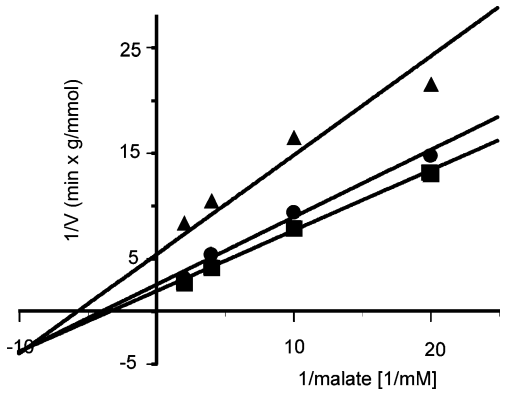

Fig. 9 Two-substrate analysis of the malate influx in the presence of internal oxoglutarate, catalyzed by the reconstituted OGC. Double reciprocal plot showing the dependence of uptake rate on the external concentrations. [^{14}C]malate was added at the concentrations of 0.05, 0.1, 0.25 and 0.5 mM to proteoliposomes containing 6 (■), 3.5 (●) and 1 mM (▲) oxoglutarate. The rate of uptake is measured in 2 min

means of second order plots, in order to compare the kinetics of the two exchange processes.

To complete the analysis of the behaviour of the carrier with respect to its substrates, the exchange between external oxoglutarate and internal malate was studied by following the influx of labelled oxoglutarate, according to the previous criterion (Figs. 11 and 12). Again, a modified Eq. (1) has been used by introducing the internal concentration of malate (B_i instead of A_i, as well K_{Bi} and k_{-4} replacing K_{Ai} and k_{-2}), and the corresponding parameters have been calculated.

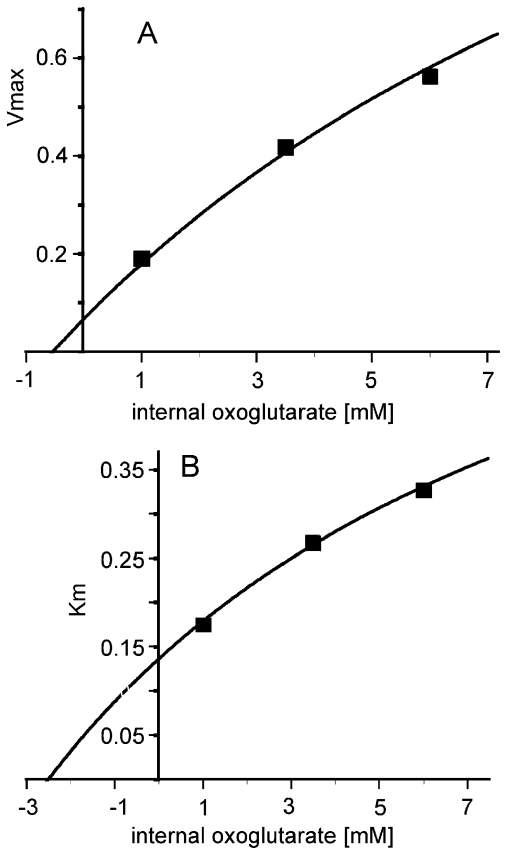

Fig. 10 Second-order plots of the data of Fig. 9. Dependence of the V_{max} (**a**) and K_m (**b**) on the internal oxoglutarate concentrations

Discussion

Kinetic mechanism

The elaboration of the experimental data presented in Figs. 5, 6, 7, 8, 9, 10, 11 and 12 allows the calculation of significant values for the parameters present in the equations, that in our hypothesis describe the transport process. As regards the kinetic constants, we cannot obtain absolute values but relative ones. In fact, we refer them to k_{-3}, whose value is imposed as one (because it resulted to be the lowest with respect to the others). Table 2 shows the results of such an elaboration from each experiment.

The values of the parameters and, much more significantly, the relationships among them obtained from the experiments reported are satisfactorily reproduced in similar experiments. So, even with some uncertainty about the absolute values, we can attempt to arrive at some conclusions from these data about the behaviour of the carrier with respect to its substrates. First, the kinetic constants of the rearrangement steps of the carrier bringing its "empty" binding site from the outside to the inside (k_3), and *vice versa* (k_{-3}), are lower than the others (with the exception of k_{-4},which is lower, or at least similar, to k_3) but not negligible. This means that such steps exert a significant influence on the transport mechanism, as is verified in the double-substrate exchange experiments,

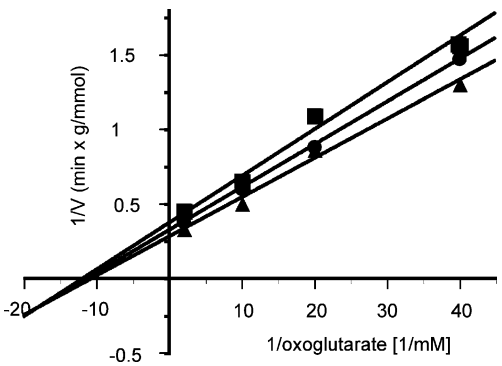

Fig. 11 Two-substrate analysis of the oxoglutarate influx in the presence of internal malate, catalyzed by the reconstituted OGC. Double reciprocal plot showing the dependence of the uptake rate on the external concentrations. [^{14}C]oxoglutarate was added at the concentrations of 0.025, 0.05, 0.1 mM and 0.5 mM to proteoliposomes containing 3 (■), 6 (●) and 9 mM (▲) malate. The rate of uptake is measured in 2 min

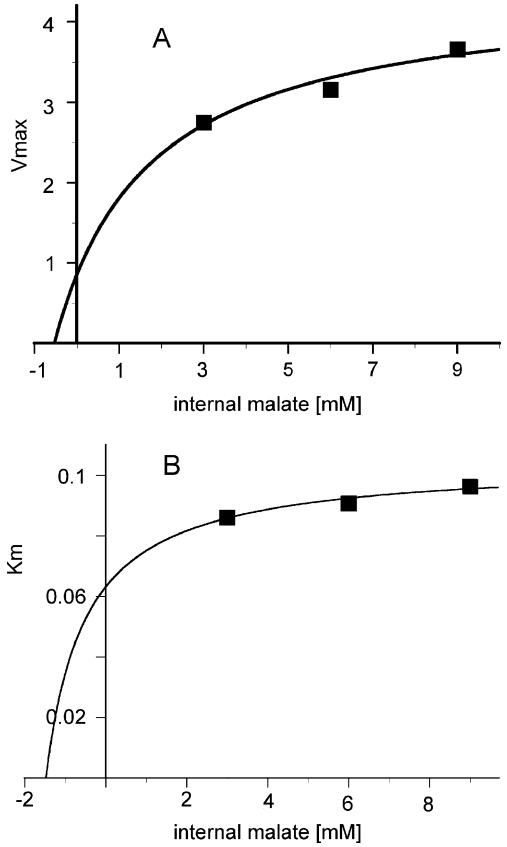

Fig. 12 Second-order plots of the data of Fig. 11. Dependence of the V_{max} (**a**) and K_m (**b**) on the internal malate concentrations

where the lines obtained at different internal concentrations meet at well defined points.

This allows us to exclude the hypothesis of an obligatory 1:1 exchange. In fact, such a hypothesis would mean that k_3 and k_{-3} would be both negligible with respect to the other kinetic constants, leading to a simplified Eq. (1) and its derived, where k_3 and k_{-3} would be absent and consequently the lines at different internal concentrations should be parallel.

Secondly, the values found for the dissociation constants indicate that the affinity of the carrier for oxoglutarate on the internal side is two orders of magnitude lower with respect to the external, while the affinity for malate is very similar on both sides.

Table 2 Kinetic and equilibrium constants of the transport process

k		K	mM
k_4	45	K_{Be}	1
k_{-4}	3	K_{Bi}	2
k_2	9	K_{Ae}	0.07
k_{-2}	26	K_{Ai}	13
k_3	5		
k_{-3}	1		

The values of the kinetic constants are relative to k_{-3}
The equilibrium constants are expressed in mM

Furthermore, we have to consider that, once a suitable value to each of the kinetic parameters and dissociation constants is detained, we will have a tool to theoretically calculate the rates of influx and efflux of any substrate at any concentration. In the simple case of the oxoglutarate/oxoglutarate exchange, under the experimental conditions used (internal concentration much higher than the external concentration), while we measure the rate of influx of labelled substrate, we expect, and can theoretically evaluate, a higher efflux of cold substrate.

While the influx rate is expressed by Eq. (1), the efflux rate is given by:

$$\overleftarrow{v} = k_{-2} \cdot CA_i = k_{-2} \cdot C_T \cdot \frac{k_2 A_e + k_3 K_{Ae}}{(k_{-2} + k_2)A_e + (k_{-2} + k_3)K_{Ae}} \cdot \frac{A_i}{A_i + \frac{(k_{-3}+k_2)A_e + (k_{-3}+k_3)K_{Ae}}{(k_{-2}+k_2)A_e + (k_{-2}+k_3)K_{Ae}} K_{Ai}} \quad (4)$$

Once the equilibrium is reached, isotopic dilution will be complete while internal and external concentrations will have changed so that influx and efflux rates compensate each other. By using the rate equations for influx and efflux of oxoglutarate we are able to calculate the equilibrium concentrations, i.e. the concentrations at which the efflux rate equals the influx rate. For example, starting from the condition in Fig. 2 (A_i=10 mM, A_e=0.1 mM), at equilibrium we obtain that A_i=4.33 mM and A_e= 0.34 mM, with a final concentration ratio decreased from 100 to about 13 (in the case of the obligatory 1:1 exchange the ratio would remain the same). It should be noted that if we start from different internal and external concentrations those at equilibrium will change but the concentration ratio must remain constant. In fact, when $\overrightarrow{v} = \overleftarrow{v}$, the result is that:

$$\frac{A_i}{A_e} = \frac{k_2 k_{-3} K_{Ai}}{k_{-2} k_3 K_{Ae}}$$

An analogous consideration holds for malate (substrate B) for which a different equilibrium concentration ratio is calculated (about 6).

$$\frac{B_i}{B_e} = \frac{k_4 k_{-3} K_{Bi}}{k_{-4} k_3 K_{Be}}$$

In the presence of both substrates, it can be demonstrated that each does not significantly modify the equilibrium concentration ratio of the other. This explains the lower equilibrium level of malate curve with respect to that of oxoglutarate (Fig. 2).

Finally, it must be considered that the pattern of kinetic plots obtained from the experimental data is typical of the proposed mechanism of uniport exchange. In fact it can be demonstrated that models bound to sequential mechanisms, with the formation of ternary complexes, lead to different equations and as a consequence to different sets of plots, which our experimental data do not fit to.

Physiological role of the carrier in the brain

The presence of the OGC in the membrane of brain mitochondria is presumably due to its role in the malate/aspartate shuttle that transfers reducing equivalents from cytosolic NADH to mitochondrial NAD^+ during the glycolytic process. In this case, its function would essentially be to exchange cytosolic malate with mitochondrial oxoglutarate and, actually, the characteristics described by the parameters in Table 2 are consistent with such a function. In fact, the kinetic constants for the uptake of malate and the efflux of oxoglutarate are the highest with respect to the others (k_4=45 and k_{-2}=26, respectively). It is not then surprising that in a simulation of the transport process using the constants in the Table 2 the highest exchange activity is accomplished with higher concentrations of external malate B_e and internal oxoglutarate A_i with respect to A_e and B_i (and not *vice versa*). Finally, one can notice that, in the simulation, the stoichiometry of the exchange between external malate and internal oxoglutarate is essentially 1:1 when the concentration ratio of internal oxoglutarate/external malate is 4–5, a finding that can have a metabolic significance.

Acknowledgments We express our gratitude to Mr. S.E. Carulli for his excellent technical work.

References

Bisaccia F, Indiveri C, Palmieri F (1985) Biochim Biophys Acta 810:362–369
Bisaccia F, Indiveri C, Palmieri F (1988) Biochim Biophys Acta 933:229–240
Bolli R, Nalecz KA, Azzi A (1989) J Biol Chem 264:18024–18030
De Palma A, Prezioso G, Scalera V (2005) J Bioenerg Biomembranes 37(5):279–287
Dulley JR, Grieve PA (1975) Anal Biochem 64:136–141
Indiveri C, Dierks T, Krämer R, Palmieri F (1991) Eur J Biochem 198:339–347
Laemmli K (1970) Nature 227:680–685
Morrissey JH (1981) Anal Biochem 117:307–310
Palmieri F (2004) Pflugers Arch 447:689–709
Palmieri F, Indiveri C, Bisaccia F, Iacobazzi V (1995) Methods Enzymol 260:349–369
Runswick MJ, Walker JE, Bisaccia F, Iacobazzi V, Palmieri F (1990) Biochemistry 29:11033–11040
Spagnoletta A, De Palma A, Prezioso G, Scalera V (2008) J Biochem Biophys Methods 70:954–957
Walker JE, Runswick MJ (1993) J Bioenerg Biomembr 25:435–446